

# AUTOMATIC GENERATION CONTROL OF INTERCONNECTED POWER SYSTEM USING ANN TECHNIQUE BASED ON $\mu$ -SYNTHESIS

Hossein Shayeghi\* — Heidar Ali Shayanfar\*\*

This paper presents a nonlinear Artificial Neural Networks (ANN) controller based on  $\mu$ -synthesis for Automatic Generation Control (AGC) of power systems. Power systems such as other industrial plants have some uncertainties and deviations due to multivariable operating conditions and load changes. For this reason, in the design of ANN controller the idea of  $\mu$  synthesis theory is used. The motivation of using the  $\mu$ -based robust controller for training the proposed controller is to take the large parametric uncertainties and modeling error into account in such a way that both the stability of the overall system and good performance have been achieved for all admissible uncertainties. The simulation results on a two-area power system show that the proposed ANN controller is effective and gives good dynamic responses even in the presence of Generation Rate Constraints (GRC). In addition, it is superior to the conventional PI and  $\mu$ -based robust controllers.

**Key words:** AGC, Power System Control, ANN,  $\mu$ -synthesis, Robust Control.

## 1 INTRODUCTION

Automatic Generation Control (AGC) is one of the most important issues in electric power system design and operation. The objective of the AGC in an interconnected power system is to maintain the frequency of each area and to keep tie-line power close to the scheduled values by adjusting the MW outputs the AGC generators so as to accommodate fluctuating load demands. The automatic generation controller design with better performance has received considerable attention during the past years and many control strategies have been developed [1-4] for AGC problem.

The availability of an accurate model of the system under study plays a crucial role in the development of the most control strategies like optimal control. However, an industrial process, such as a power system, contains different kinds of uncertainties due to changes in system parameters and characteristics, loads variation and errors in the modeling. On the other hand, the operating points of a power system may change very much randomly during a daily cycle. Because of this, a fixed controller based on classical theory [3-4] is certainly not suitable for AGC problem. Thus, some authors have suggested a variable structure [5-7] and neural networks methods [8-9] for dealing with parameter variations. All the proposed methods are based on the state-space approach and require information about the system states which are not usually known or available.

On the other hand, various adaptive techniques [10-11] have been introduced for AGC controller design. Due to the requirement of a perfect model which has to track the state variables and satisfy system constraints, it is

rather difficult to apply these adaptive control techniques to AGC in practical implementations. Recently, several authors have applied robust control methodologies [12-15] to the solution of AGC problem. Although via these methods, the uncertainties are directly introduced to the synthesis. But models of large scalar power systems have several features that preclude direct application of robust control methodologies. Among these properties, the most prominent are: very high (and unknown) model order, uncertain connection between subsystems, broad parameter variation and elaborate organizational structure.

In this paper, because of the inherent nonlinearity of power systems we address a new nonlinear Artificial Neural Network (ANN) controller based on  $\mu$ -synthesis technique. The motivation of using the  $\mu$ -based robust controller for training the proposed controller is to take the large parametric uncertainties and modeling error into account. To improve the stability of the overall system and also its good dynamic performance achievement, the ANN controller has been reconstructed with applying the  $\mu$ -based robust controller to power systems in different operating points under different load disturbances by using the learning capability of the neural networks. Moreover, the proposed controller also makes use of a piece of information which is not used in the conventional and  $\mu$ -based robust controllers (an estimate of the electric load perturbation, *ie* an estimate of the change in electric load when such a change occurs on the bus). The load perturbation estimate could be obtained either by a linear estimator or by a nonlinear neural network estimator in certain situations. It could also be measured directly from the bus. We will show by simulation that when a load estimator is available, the ANN controller can achieve an extremely

\* Technical Engineering Department, Mohaghegh University, Ardebil, Iran, h.shayeghi@yahoo.com

\*\* Electrical Engineering Department, Iran University of Science and Technology, Tehran, Iran, shayanfar@hotmail.com.

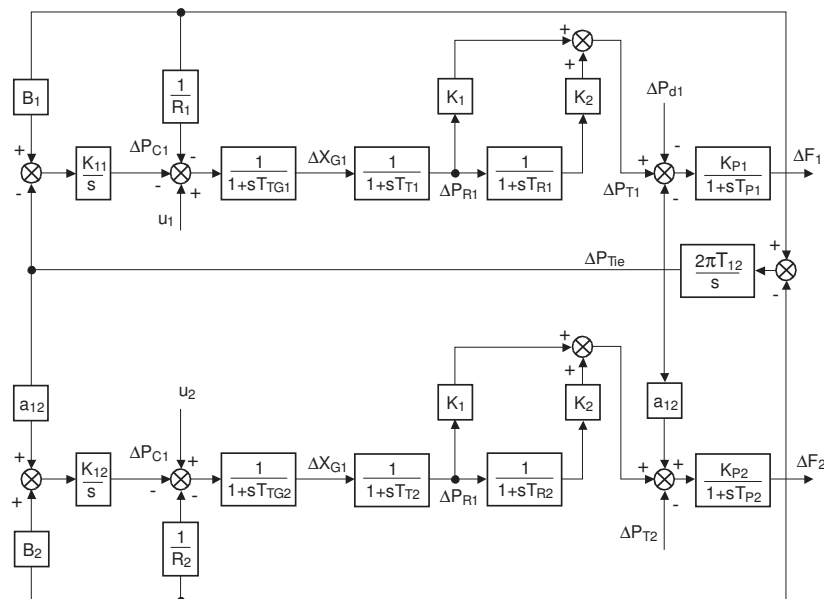


Fig. 1. Block diagram of a two-area power system

dynamic response. In the work, a two-area power system is considered as a test system. Each area of the power system consists of steam turbines, which include reheaters. Therefore, there are the effects of reheaters and generating rate boundaries in each area. For comparison, the considered system is controlled by using:

- (i) Conventional integral controller
- (ii)  $\mu$ -based robust controller
- (iii) ANN controller

for different cases of the plant parameter changes under various step load disturbances. The simulation results show that the proposed controller is very effective and gives a good dynamic response compared to the conventional PI and  $\mu$ -based robust controllers even in the presence of the plant parameters changes and Generation Rate Constraint (GRC).

## 2 PLANT MODEL

A large power system consists of a number of interconnected control areas connected by tie-lines power. There are different complicated nonlinear models for large-scale

power systems. However, for the design of AGC a simplified and linearized model is usually used [16]. In advanced control strategies (such as the one considered in this paper) the errors caused by simplification and linearization are considered as parametric uncertainties and unmodeled dynamics. A two-area power system is taken as a test system in this study. In each area, all generators are assumed to be a coherent group. Figure 1 shows the block diagram of the system in detail. Each area including the steam turbine contains a governor, reheater stage of the steam turbine. The governor dead-bound effects that are important for speed control under small disturbances are considered to be 0.06% [1]. The nomenclature used and the nominal parameter values are given in Appendix A.

The state space model for the system of Fig. 1 can be constructed as:

$$\begin{aligned} \dot{\mathbf{x}} &= \mathbf{A}\mathbf{x} + \mathbf{B}_1\mathbf{u} + \mathbf{F}\mathbf{d} \\ \mathbf{y} &= \mathbf{C}\mathbf{x} \end{aligned} \tag{1}$$

where

$$\begin{aligned} \mathbf{u} &= [u_1 \ u_2]^T; \quad \mathbf{d} = [\Delta P_{d1} \ \Delta P_{d2}]^T, \\ \mathbf{y} &= [\Delta F_1 \ \Delta P_{Tie} \ \Delta F_2]^T, \quad \mathbf{x} = [\Delta P_{C1} \ \Delta X_{G1} \ \Delta P_{R1} \\ &\quad \Delta P_{T1} \ \Delta F_1 \ \Delta P_{Tie} \ \Delta P_{C2} \ \Delta X_{G2} \ \Delta P_{R2} \ \Delta P_{T2} \ \Delta F_2]^T, \end{aligned}$$

$$\mathbf{A} = \begin{bmatrix} 0 & 0 & 0 & 0 & K_{I1}B_1 & K_{I1} & 0 & 0 & 0 & 0 & 0 \\ -1/T_{G1} & -1/T_{G1} & 0 & 0 & -1/R_1T_{G1} & 0 & 0 & 0 & 0 & 0 & 0 \\ 0 & 1/T_{T1} & -1/T_{T1} & 0 & 0 & 0 & 0 & 0 & 0 & 0 & 0 \\ 0 & K_1/T_{T1} & a & -1/T_{R1} & 0 & 0 & 0 & 0 & 0 & 0 & 0 \\ 0 & 0 & 0 & K_{P1}/T_{P1} & -1/T_{P1} & -K_{P1}/T_{P1} & 0 & 0 & 0 & 0 & 0 \\ 0 & 0 & 0 & 0 & 2\pi T_{12} & 0 & 0 & 0 & 0 & 0 & -2\pi T_{12} \\ 0 & 0 & 0 & 0 & -K_{I2} & 0 & 0 & 0 & 0 & -K_{I2}B_2 & 0 \\ 0 & 0 & 0 & 0 & 0 & 0 & -1/T_{G2} & -1/T_{G2} & 0 & 0 & -1R_2T_{G2} \\ 0 & 0 & 0 & 0 & 0 & 0 & 0 & 1/T_{T2} & -1/T_{T2} & 0 & 0 \\ 0 & 0 & 0 & 0 & 0 & 0 & 0 & K_2/T_{T2} & b & -1/T_{R2} & 0 \\ 0 & 0 & 0 & 0 & 0 & K_{P2}/T_{P2} & 0 & 0 & 0 & K_{P2}/T_{P2} & -1/T_{P2} \end{bmatrix},$$

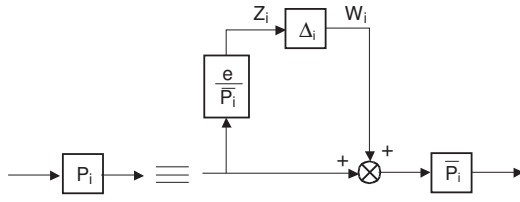


Fig. 2. The parametric uncertainty model

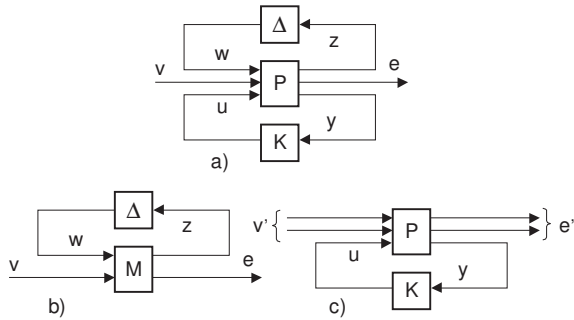

 Fig. 3.  $\mu$  Analysis and synthesis structure: (a) general interconnected structure, (b) analysis, (c) synthesis

Table 1. Parametric uncertainties of the system

$P_i$	$P_{Li}$	$\bar{P}_i$	$P_{Ui}$	$\varepsilon$
$B_i$	0.34	0.43	0.52	0.09
$1/T_{Gi}$	8.33	10.42	12.5	2.07
$1/R_i T_{Gi}$	2.983	4.7	6.51	1.81
$1/T_{Ti}$	2.78	3.4735	4.167	0.6935
$1/T_{Ri}$	0.0833	0.1042	0.125	0.0208
$K_{Pi}/T_{Pi}$	4	8	12	4
$1/T_{Pi}$	0.033	0.0665	0.1	0.0335
$T_{12}$	0.049	0.0707	0.093	0.0223

$$a = (K_1 + K_2)/T_{T1} - K_2/T_{R1},$$

$$b = (K_1 + K_2)/T_{T2} - K_2/T_{R2},$$

$$B_1 = \begin{bmatrix} 0 & 1/T_{G1} & 0 & 0 & 0 & 0 & 0 & 0 & 0 & 0 & 0 \\ 0 & 0 & 0 & 0 & 0 & 0 & 0 & 1/T_{G2} & 0 & 0 & 0 \end{bmatrix},$$

$$F = \begin{bmatrix} 0 & 0 & 0 & 0 & -K_{P1}/T_{P1} & 0 & 0 & 0 & 0 & 0 & 0 \\ 0 & 0 & 0 & 0 & 0 & 0 & 0 & 0 & 0 & -K_{P2}/T_{P2} & 0 \end{bmatrix},$$

$$C = \begin{bmatrix} 0 & 0 & 0 & 0 & 1 & 0 & 0 & 0 & 0 & 0 & 0 \\ 0 & 0 & 0 & 0 & 0 & 1 & 0 & 0 & 0 & 0 & 0 \\ 0 & 0 & 0 & 0 & 0 & 0 & 0 & 0 & 0 & 0 & 1 \end{bmatrix}.$$

## 2.1 Parametric uncertainty and description

Parameters of the linear model described for the AGC problem in Fig. 1 depend on the operating points. On the other hand, because of the inherent characteristics of loads changing and system configuration, the operating points of the power system may change very much randomly during a daily cycle. Thus, the real power system will contain parametric uncertainty such as other industrial plants. First, we show a way how to consider the

change of each parameter. Denoting  $i$ -th certain parameter by  $P_i$  the parameter uncertainty is formulated as:

$$\bar{P}_i - \varepsilon \leq P_i \leq \bar{P}_i + \varepsilon \text{ or } P_i = \bar{P}_i \left( 1 + \frac{\varepsilon}{\bar{P}_i} \Delta_i \right), |\Delta_i| \leq 1. \quad (2)$$

Here  $\bar{P}_i$  is the nominal value of the parameter and  $\varepsilon$  the upper bound of  $P_i$  its variation. Therefore, we can separate  $\Delta$  that represents the variation element as shown in Fig. 2.

Table 1 shows the eight parametric uncertainties of the system described in section 2 with their nominal, upper and lower bound values, where  $P_{Ui}$  and  $P_{Li}$  stand for the upper and lower bound values, respectively. The range of parameters variation are obtained by simultaneously changing  $T_P$ ,  $T_{12}$  by 50% and all other parameters by 20% of their typical values as given in Appendix A.

Now let us define:

$$B = [F \quad B_1], \quad \mathbf{u}_1^T = [d^T \quad \mathbf{u}^T], \quad (3)$$

With these definitions and due to Eq. (2), the state space model of the system becomes:

$$\dot{\mathbf{x}} = \left( \mathbf{A}_0 + \sum_{i=1}^8 \delta_i \mathbf{A}_i \right) \mathbf{x} + \left( \mathbf{B}_0 + \sum_{i=1}^8 \delta_i \mathbf{B}_i \right) \mathbf{u}_1, \quad (4)$$

$$\mathbf{y} = \mathbf{C} \mathbf{x}.$$

The  $\mathbf{A}_0$  and  $\mathbf{B}_0$  matrices are obtained by substituting nominal values of the system parameters into the matrices  $\mathbf{A}$  and  $\mathbf{B}$  defined above. The matrices  $\mathbf{A}_i$  and  $\mathbf{B}_i$  are obtained by differentiating the matrices of  $\mathbf{A}$  and  $\mathbf{B}$  with respect to the  $i$ -th uncertainty, respectively.

## 3 STRUCTURE SINGULAR VALUE AND $\mu$ -BASED AGC CONTROLLER DESIGN

This section gives a brief overview of structure singular value. Also, the procedure of the  $\mu$ -based AGC controller design is given.

### 3.1. Structure singular value and $\mu$ synthesis

The general framework of  $\mu$  analysis and synthesis [17] shown in Fig. 3 is based on the Linear Fractional Transformations (LFTs). Any linear interconnection of inputs, outputs and commands along with perturbations and a controller can be viewed in this context and rearranged to match this diagram. For the purpose of analysis, controller  $K$  is obtained into plant  $P$  to form the interconnected structure in Fig. 3(b). Given an uncertainty with known structure, bounded value and belonging to the set  $B\Delta$ :

$$\Delta = \{diag(\delta_1 I_{r1}, \dots, \delta_s I_{rs}, \Delta_1, \dots, \Delta_F);$$

$$\delta_i \in C, \Delta_j \in C^{m_i \times m_j}\}, \quad (5)$$

$$B\Delta = \{\Delta \in \Delta | \bar{\sigma}(\Delta) \leq 1\}.$$

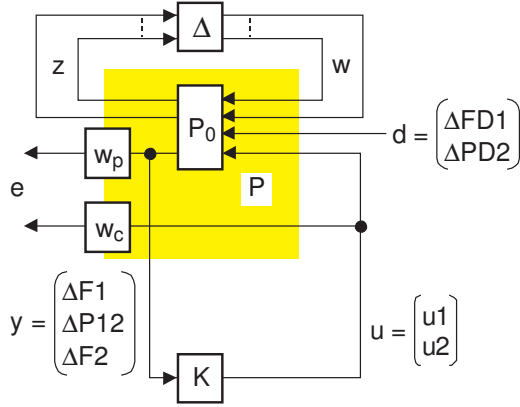


Fig. 4.  $\mu$  controller design problem formulation

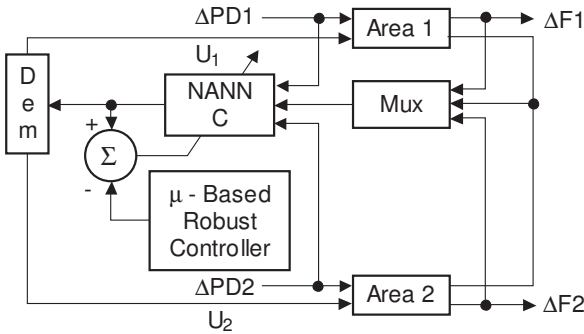


Fig. 5. Block diagram of the NANN controller design

For a system described in the complex matrix,  $\mathbf{M} \in \mathbb{C}^{n \times n}$ , the structural singular value  $\mu$  is defined as:

$$\mu_{\Delta}(\mathbf{M}) = \frac{1}{\min\{\sigma(\Delta) : \Delta \in \Delta, \det(\mathbf{I} - \mathbf{M}\Delta) = 0\}} \quad (6)$$

Thus,  $\mu_{\Delta}(\mathbf{M})$  is a measure of the smallest structured  $\mu$  that causes instability of the constant matrix feedback loop shown in Fig. 3(b). Given a desired uncertainty level, the purpose of this design is to look for a control law which can bring down the closed loop system  $\mu$  level and ensure the stability of the system for all possible uncertainty descriptions.

The performance and stability conditions for a system in the presence of structured uncertainty in terms of  $\mu$  are given as:

1. Robust stability (RS)

$$F_u(M, \Delta) \text{ stable } \forall \Delta \in B\Delta \quad \text{iff } \sup_{\omega} \mu(M_{11}(j\omega)) \leq 1. \quad (7)$$

2. Robust performance (RP)

$$F_u(M, \Delta) \text{ stable } \& \|F_u(M, \Delta)\|_{\infty} \leq 1 \quad \forall \Delta \in B\Delta \\ \text{iff } \sup_{\omega} \mu(M(j\omega)) \leq 1. \quad (8)$$

In other words, the performance and stability of the closed loop system  $M$  is a  $\mu$  test, across frequency for the given uncertainty structure  $\Delta$ .

The synthesis problem is represented by the structure in Fig. 3(c). The control error  $e'$  can be expressed as the following LFT.

$$e' = F_L(P, K)v' = [P_{11} + P_{12}K(I - P_{22}K)^{-1}P_{21}]v'. \quad (9)$$

Ideally, the goal is to find a controller  $K$  such that:

$$\|F_L(P, K)\|_{\mu} \leq 1.$$

However, as there is no effective technique to which this  $K$  is obtained directly at present, indirectly it is calculated by  $K$  and scaling matrix  $D$  until Eq. (10) is fulfilled:

$$\min_K \inf_D \|DF_L(P, K)D^{-1}\|_{\infty} \leq 1, \quad (10) \\ D = \{diag(d_1I, d_2I, \dots, d_nI) \mid d_i \in R_+\}.$$

In the minimization, fixing either  $D$  or  $K$  is called especially  $D$ - $K$  iteration [18]. It does not become a trouble so much in practice use, and is widely used.

3.2  $\mu$ -Based AGC controller design for AGC

The objective of the controller design in an interconnected power system is damping of the frequency and tie-line power deviations oscillations, stability of the overall system for all admissible uncertainties and load changes. Thus, frequency and tie-line power deviations ( $\Delta F_1, \Delta P_{tie}, \Delta F_2$ ) in two areas power system are considered as controller inputs. The first step in designing the  $\mu$ -based controller is to formulate design problem into  $\mu$  general framework. By using Eq. (4) and following the procedure of Ref. [1], the state-space model along with uncertainties model will be separated as:

$$P_0: \begin{cases} \dot{x} = A_0x + B_0u_1 + B_1w, \\ z = C_zx + D_zu_1, \\ y = Cx, \\ w = \Delta z. \end{cases} \quad (11)$$

Here the structured uncertainty block is:

$$\Delta = \{diag(\delta_1I_2, \dots, \delta_7I_2, \delta_8); \delta_i \in R, \|\Delta\| \leq 1\}.$$

The design problem formulation into the  $\mu$  general structure is shown in Fig. 4. In this diagram,  $P_0$  is the interconnection of the nominal plant and all parametric uncertainties. In order to take the modelling error into account, an additional input multiplicative uncertainty is considered by weighting function  $W_C$ . The  $W_P$  also indicates the system performance specifications. The weights have been selected based on Ref. [14] as:

$$W_C(s) = \frac{0.33s + 1.5}{30s + 0.33}, \quad (12)$$

$$W_P(s) = \frac{0.7}{1.245s + 0.007} \cdot \frac{s + 1.245}{s + 0.007}. \quad (13)$$

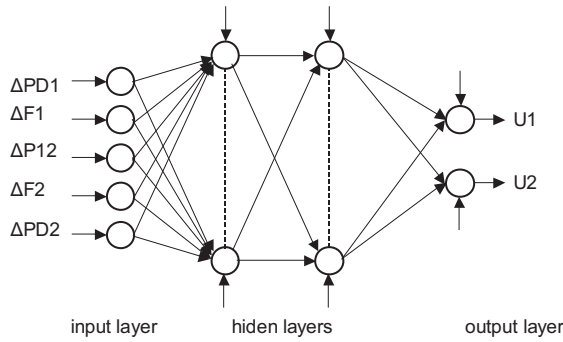


Fig. 6. The artificial neural network architecture

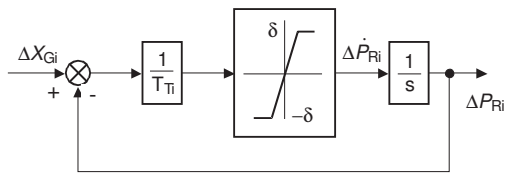


Fig. 7. A nonlinear turbine model with GRC

All above components are compressed into a generalized plant  $P$  to perform the  $\mu$  analysis. A software tool [19] has been used for the design of  $\mu$ -based AGC controller. The control law obtains in the form of state space notation  $A_K$ ,  $B_K$  and  $C_K$  with system order 106. It should be noted, although via  $\mu$  synthesis the uncertainty can be introduced to the controller synthesis, but due to the high model order of power systems the order of the obtained controller will be very high in general.

#### 4 THE ANN CONTROLLER DESIGN FOR AGC

##### 4.1 The ANN Features

Recently, computational intelligence systems and among them neural networks, which in fact are model free dynamics, have been used widely for approximation functions and mappings. The main feature of neural networks is their ability to learn from samples and generalizing them and also their ability to adapt themselves to the changes in the environment. In fact, neural networks are very suitable for problems in the real world. These networks with participation of a special kind of parallel processing are able to provide the modeling of any kind of nonlinear relations. Higher accuracy, robustness, generalized capability, parallel processing, learning static and dynamic model of MIMO systems on collected data and its simple implementation are some of the importance characteristics of the neural network that caused wide applications of this technique in different branches of sciences and industries, especially in designing of the nonlinear control systems [9, 20]. The salient feature of artificial intelligent technique is that they provide a model-free description of control systems and do not require the accurate model of the plant. Thus, they are very suitable

for control of the nonlinear plants that their models are unknown or have uncertainty such as a large scale power system.

##### 4.2 The $\mu$ -based ANN Controller

There are some deviations and uncertainties due to changes in system parameters, characteristics and load variations in power systems that for the controller design have to be considered. On the other hand, very high (and unknown) model order, uncertain connection between subsystems, broad parameter variations and elaborate organizational structure of the power system preclude direct application of standard robust control methodologies. In order to overcome this drawback, we propose a new Nonlinear Artificial Neural Network (NANN) controller based on  $\mu$ -synthesis technique. Figure 5 shows the designing procedure of the NANN proposed controller for two-area power system. The Multi Layer Perceptron (MLP) neural networks for the design of the nonlinear AGC controller in two areas power systems are being used.

Since the objective of AGC controller design in an interconnected power system is damping of the frequency and tie-line power deviations and in such a way minimizing transient oscillation under different load conditions. Thus, frequency and tie-line power deviations are chosen as the neural network controller inputs. Moreover, in order to evaluate the control signal ( $u$ ), the NANN controller is using a piece of information which is not used in the conventional and modern controller (an estimate of the load perturbation  $\Delta \hat{P}D_i$ ). In general, the load perturbation of the large system is not directly measurable. Therefore, it must be estimated by a linear estimator or by a nonlinear neural network estimator, if the nonlinearities in the system justify it. Such an estimator takes as inputs a series of  $k$  samples of the frequency fluctuations at the output of the generator  $[\Delta F(n)\Delta F(n-1)\dots\Delta F(n-k+1)]^T$  and estimates the instantaneous value of the load perturbation based on this input vector. The implementation of such an estimator is beyond the scope of this paper. Here, we assume that the load estimate  $\Delta \hat{P}D_i$  is available, i.e.  $\Delta \hat{P}D(n) = \Delta PD(n)$ .

##### 4.3 Neural Network Architecture and Training

The NANN controller architecture employed here is a MLP neural network, which is shown in Fig. 6. The frequency deviations, tie-line power deviation and load perturbation of each area are chosen as the neural network controller inputs. The outputs of the neural network are the control signals, which are applied to the governors in each area. The data required for the NANN controller training is obtained from the designing and applying the  $\mu$ -based robust controller to power system in different operating points with various load disturbances.

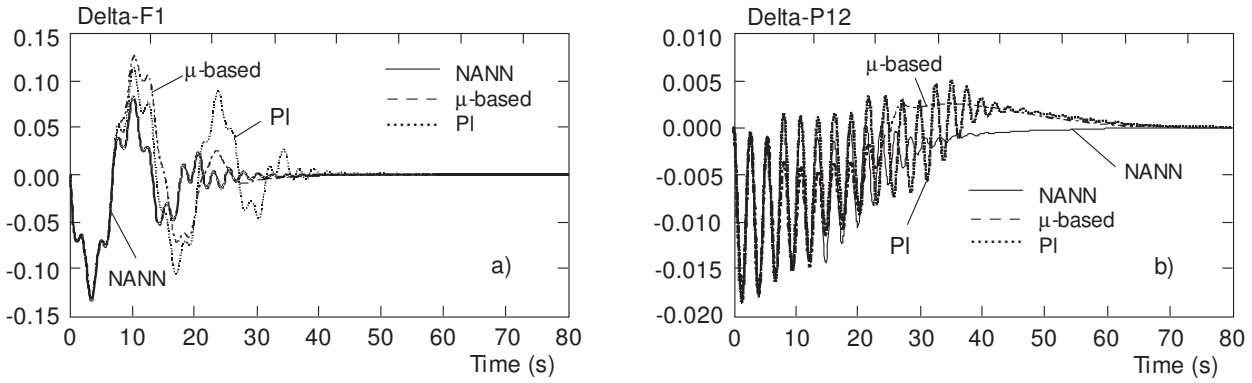


Fig. 8. The performance of the controllers for the case A: a) The responses of frequency deviations, b) The responses of tie-line power deviations

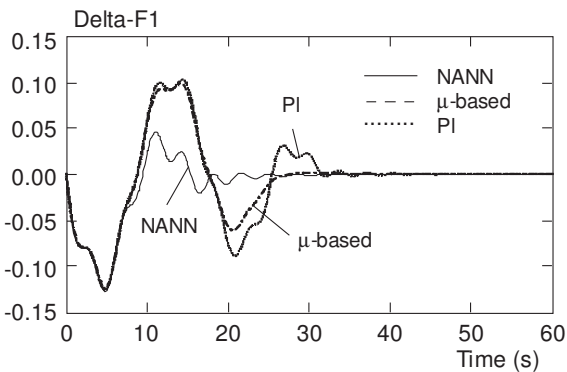


Fig. 9. The performance of the controllers for the case B

After a series of trial and error and modifications, the ANN architecture shown in Fig. 6 provides the best performance. It is a four-layer perceptron with 5 inputs, 15 neurons in the first hidden layer, 7 neurons in the second hidden layer and two outputs. The activation function of the networks neurons is hyperbolic tangent. The proposed network has been trained by using back-propagation algorithm [20]. The Root Mean Square (RMS) error criterion is being used to evaluate the learning performance. Learning algorithms cause the adjustment of the weights so that the controlled system gives the desired response.

### 5 SIMULATION RESULTS

The test system for AGC as shown in Fig. 1 consists of two areas control, and its parameters are given in Appendix A. The considered system is controlled by using: 1) conventional integral controller; 2)  $\mu$ -based robust controller designed according to the procedure described in section 3; and 3) the nonlinear ANN controller designed based on the procedure presented in section 4. These results show that the structure of ANN controller is simpler than the  $\mu$ -based robust controller whereas order of  $\mu$ -based controller is very large that is caused this control strategy is difficult in practical implementations.

One of the importance constraints in AGC of the power system is Generation Rate Constraints (GRC),

ie the practical limit on the rate of change in the generating power. The results in Refs. [21, 22] indicated that GRC would influence the dynamic responses of the system significantly and lead to larger overshoot and longer settling time. Furthermore, since the system parameters are unknown, the overall system may become unstable in the presence of a load disturbance. In order to take effect of the GRC into account, in the simulation study, the linear model of a turbine  $\Delta P_R/\Delta X_G$  in Fig. 1 is replaced by a nonlinear model of Fig. 7. The GRC is 0.2 pu per minute ( $\delta = 0.005$ ) is considered [21]. Also, two limiters, bounded by  $\pm 0.005$ , are used within the above controller to prevent the excessive control action. They limit the following control signals:

$$|\dot{u}_i(t)| \leq 0.005, \quad |\Delta \dot{P}_{Ci}(t)| \leq 0.005.$$

In this section, the performance of ANN controller is compared with the conventional and  $\mu$ -based controllers for four cases of the plant parameters changes and load disturbances.

*Case A:* We will test the system performance with nominal parameters. We choose the nominal parameters as given in Appendix A and apply load changes of  $\Delta P_{d1}(t) = 0.02$  p. u. MW to one area. The responses of  $\Delta F_1(t)$  and  $\Delta P_{tie}(t)$  are shown in Fig. 8. From these results, it can be seen that the frequency and tie-line power deviations effectively damped to zero with NANN controller.

*Case B:* We choose the lower-bound parameters as given in Table 1 for two areas and apply load changes of  $\Delta P_{d1}(t) = 0.02$  and  $\Delta P_{d2}(t) = 0.005$  pu MW to one and two areas. The responses of  $\Delta F_1(t)$  is depicted in Fig. 9. The simulation results indicated that NANN controller has better performance than to other controllers.

*Case C:* We choose the upper-bound parameters for two areas as given in Table 1 and apply load changes of  $\Delta P_{d1}(t) = 0.02$  and  $\Delta P_{d2}(t) = 0.008$  pu MW to one and two areas. The responses of  $\Delta F_1(t)$  and  $\Delta P_{tie}(t)$  are depicted in Figs. 10(a) and (b). From these results, it can be seen that NANN controller achieves good dynamic responses.



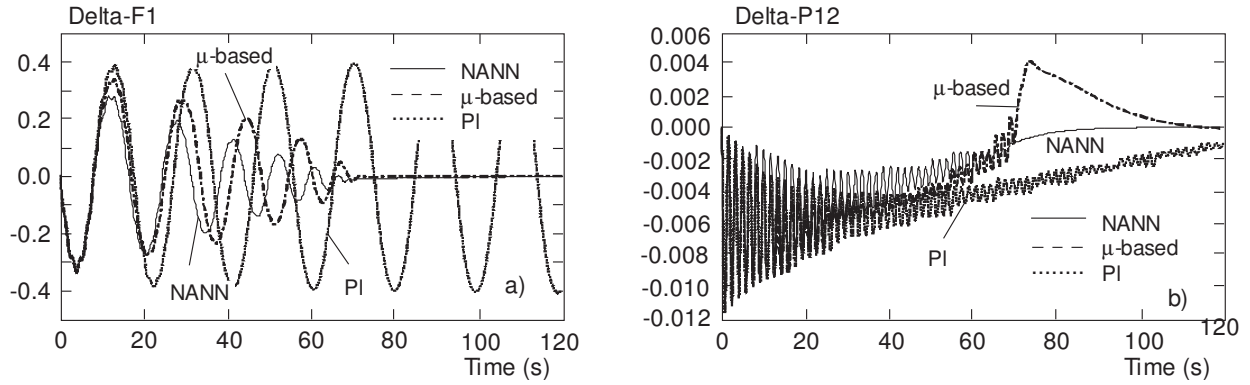


**Fig. 10.** The performance of the controllers for the case C: a) The responses of frequency deviations, b) The responses of tie-line power deviations

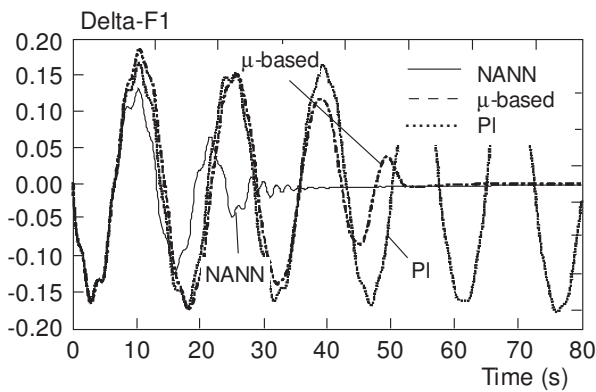


**Fig. 11.** The performance of the controllers for the case D

*Case D:* We choose the nominal values for all parameters except the plant gain  $K_{P_i} = 180$  for two areas and apply load changes of  $\Delta P_{d1}(t) = 0.015$  and  $\Delta P_{d2}(t) = 0.005$  pu MW to one and two areas. The responses of  $\Delta F_1(t)$  are depicted in Fig. 11. The simulation results indicated that NANN controller is superior to other controllers.

**Remark 5.1.** The worst case, as seen from all the simulation results, occurs when two areas are using upper bound parameters and having simultaneous load disturbances.

**Remark 5.2.** From the simulation results in Fig. 11, we can see that the responses of overall system are more sensitive to the plant gain  $K_{P_i}$  than to other parameters.

**Remark 5.3.** We have considered different cases for AGC control of a two-area power system. The simulation results indicated that the proposed ANN controller can guarantee the stability of the overall system and achieves good performance even in the presence of GRC.

## 6 CONCLUSION

In this paper, a new nonlinear ANN controller based on  $\mu$ -synthesis technique is proposed for the automatic generation control of large-scale power system. This control

strategy was chosen because of complexity of the actual uncertainty, multivariable operating conditions and large model order of the power system. The motivation of using the  $\mu$ -based robust controller for training of the neural network controller is to take the large parametric uncertainties and modeling error into account. To improve the controller performance, the proposed controller makes use of the load perturbation as input control signal, which is not used in the conventional PI and  $\mu$ -based robust controller. A two area power system is used as the test system with different cases of operating conditions and load disturbances. The simulation results show that the proposed ANN controller has better control performance compared to the conventional PI and  $\mu$ -based robust controllers even in the presence of GRC. In addition, it is effective and can ensure the stability of the overall system for all admissible uncertainties and load changes.

## Appendix A

### A.1 Nomenclature

- $\Delta f_i(t)$ : incremental frequency deviation in Hz
- $\Delta P_{T_i}(t)$ : incremental change in the  $i$ th subsystem's output in pu MW
- $\Delta P_{R_i}(t)$ : incremental change in the output energy of the  $i$ th reheat type turbine in pu MW
- $\Delta P_{C_i}(t)$ : incremental change in the integral controller
- $\Delta P_{T_{ie}}(t)$ : incremental change in the tie-line power
- $\Delta P_{d_i}(t)$ : load disturbance for the  $i$ th area in pu MW
- $u_i(t)$ : output of the automatic generation controller for  $i$ th area
- $T_{G_i}$ :  $i$ th governor time constant in s
- $T_{T_i}$ :  $i$ th turbine time constant in s
- $T_{R_i}$ :  $i$ th reheat time constant in s
- $T_{P_i}$ :  $i$ th subsystem-model time constant in s
- $T_{T_i}$ :  $i$ th reheat time constant in s
- $K_{P_i}$ :  $i$ th subsystem gain
- $K_{I_j}$ :  $i$ th subsystem's integral control gain

$B_i$ :  $i$ th subsystem's frequency-biasing factor  
 $K_i$ : the ratio between output energy of the  $i$ th stage of turbine to total output energy  
 $R_i$ : speed regulation for  $i$ th subsystem due to the  $i$ th governor action in Hz/pu MW  
 $T_{ij}$ : synchronizing coefficient of the tie-line between  $i$ th and  $j$ th areas  
 $a_{12}$ : the ratio between the base values of two areas

## A.2 Nominal parameters of two-area system

$T_{G1} = T_{G2} = 0.1$  s,  $T_{T1} = T_{T2} = 0.3$  s,  
 $T_{R1} = T_{R2} = 10$  s,  $T_{P1} = T_{P2} = 20$  s,  
 $K_{P1} = K_{P2} = 120$  Hz/p.u. MW,  $a_{12} = 1$ ,  
 $R_1 = R_2 = 2.4$  Hz/p.u. MW,  
 $B_1 = B_2 = 0.425$  p.u. MW/Hz,  
 $K_1 = K_2 = 0.5$ ,  $K_{I1} = K_{I2} = 0.05$ ,  $T_{12} = 0.0707$ ,

## REFERENCES

- [1] KARRARI, M.—SHAYEGHI, H.—MENHAJ, M. B.—ABEDI, M.: Design of  $H_\infty$  Controller Load Frequency Control in Electric Power Systems, *Amirkabir Journal of Science & Technology* **11** No. 41 (1999), 79–88.
- [2] FELIACHI, A.: On Load Frequency Control in a Deregulated Environment, *IEEE Inter. Conference on Control Applications*, pp. 437–441, 15–18 Sept. 1996.
- [3] NANDA, J.—KAVI, BL.: Automatic Generation Control of Interconnected Power Systems, *IEE Proc. on Gen. Tran. and Dis.* **125** No. 5 (1988), 385–390.
- [4] DAS, D.—NANDA, J.—KHOTHARI, ML.—KHOTHARI, DP.: Automatic Generation Control of Hydrothermal System with New Area Control Error Considering Generation Rate Constant, *Electric Machines and Power Systems* **18** (1990), 461–467.
- [5] JIANG, H.—CAI, H.—DORSEY, F.—QU, Z.: Toward a Globally Robust Decentralized Control for Large-Scale Power Systems, *IEEE Trans. on Control System Technology* **5** No. 3, (1997), 309–319.
- [6] BENGIAMIN, N. N.—CHAN, W. C.: Variable Structure Control of Electric Power Generation, *IEEE Trans. on PAS*, **101** (1982), 376–380.
- [7] AL-HAMOUZ, Z. M.—AL-DUWAISH, H. N.: A New Load Frequency Variable Structure Controller Using Genetic Algorithms, *Electric Power Systems Research* **55** No. 1 (2000), 1–6.
- [8] BEAUFAYS, F.—ABDEL-MAGID, Y.—WIDROW, B.: Application of Neural Networks to Load Frequency Control in Power System, *Neural Networks* **7** No. 1 (1994), 183–194.
- [9] ZEYNELGIL, H. L.—DEMIREN, A.—SENGOR, N. S.: The Application of ANN Technique to Automatic Generation Control for Multi-Area Power System, *Electrical Power and Energy Systems* **24** (2002), 545–554.
- [10] PAN, C. T.—LIAW, C. M.: An Adaptive Controller for Power System Load-Frequency Control, *IEEE Trans. on Power Systems* **4** No. 1 (1988), 122–128.
- [11] KAZEMI, M. H.—KARRARI, M.—MENHAJ, M. B.: Decentralized Robust Adaptive-Output Feedback Controller for Power System Load Frequency Control, *Electrical Engineering* **84** No. 2 (2002), 75–83.
- [12] NGAMROO, I.—MITANI, Y.—TSUJI, K.: Robust Load Frequency Control by Solid-State Phase Shifter Based on  $H_\infty$ , *Control Design IEEE Power Engineering Society Winter Meeting*, vol. 1, pp. 725–730, 1999.
- [13] KARRARI, M.—MENHAJ, M. B.: The  $H_\infty$  Theory for Interconnected Power Systems Load Frequency Control, *Proceedings of the Eighteenth International Conf. on Modeling, Identification and Control*, pp. 199–203, Innsbruck, Austria, 1999.
- [14] SHAYEGHI, H.—SHAYANFAR, H. A.:  $\mu$  Controller Design for Interconnected Power Systems Load Frequency Control, *Proc. of the Inter. Conf. on PES*, No. 352-158, pp. 751–758 California, USA, 13-15 May 2002.
- [15] SHIBATA, T.—YONEYAMA, S.—OHTAKA, T.—IWAMOTO, S.: Design of Load Frequency Control Based on  $\mu$  Synthesis, *IEEE/PES Transmission and Distribution Conference and Exhibition Asia Pacific*, vol. 3, pp. 1589–1594, 6–10 Oct. 2002.
- [16] SAADAT, H.: *Power System Analysis*, Mc Graw Hill, USA, 1999.
- [17] PACKARD, A.—DOYLE, J. C.: The Complex Structured Singular Value, *Automatica* **29** No. 1 (1993), 77–109.
- [18] BALAS, G. J.—DOYLE, J. C.—GLOVER, K.—PACKARD, A.—SMITH, R.: *The  $\mu$ -Analysis and Synthesis Toolbox for Use with Matlab*, The Mathworks Inc., South Natick, 1998.
- [19] APKARIAN, P.—CHRETIEN, J. P.:  $\mu$  Synthesis by D-K Iterations with Constant Scaling, *ACC Proc.*, pp. 3192–3196, 1993.
- [20] HAYKIN, S.: *Neural Networks – A Comprehensive Foundation*, 2nd Edition, Prentice Hall, New Jersey, 1999.
- [21] KUNDE, P.: *Power System Stability and Control*, McGraw-Hill, USA, 1994.
- [22] MOON, Y.-H.—RYU, H.-S.—LEE, J.-G.—SUNG, K.-B.—SHIN, M.-C.: Extended Integral Control for Load Frequency Control with the Consideration of Generation-Rate Constraints, *Electrical Power and Energy Systems* **24** (2002), 263–269.

Received 15 June 2004

**Hossein Shayeghi** received the BS degree in electrical engineering from KNT University of Technology in 1996, and his MSEE degree from Amirkabir University of Technology in 1998. He is currently a PhD candidate at the Iran University of Science and Technology, Tehran, Iran. His research interests are in the application of robust control, artificial intelligence to power system control design and power system restructuring.

**Heidar Ali Shayanfar** received the BS degree in electrical engineering from Iran College of Science and Technology in 1973, and his MSEE degree from Wayne State University, Detroit, MI, USA in 1979. He received PhD degree in electrical engineering from Michigan State University, E. Lansing, MI, USA in 1981. Currently, He is a Full Professor at Electrical Engineering Department of Iran University of Science and Technology, Tehran, Iran. His research interests are in the application of artificial intelligence to power system control design, dynamic load modelling, power system observability studies, voltage collapse and power system restructuring.